The University of South Bohemia in České Budějovice

Faculty of Science

Analysis of proteins putatively located in the mitochondria of *Trypanosoma brucei*

Bachelor thesis

Stina Eßmann

Advisor: Ignacio Durante, Ph.D

Co-Advisor: Mgr. Vendula Rašková

České Budějovice 2021

Eßmann S., 2021: Analysis of proteins putatively located in the mitochondria of *Trypanosoma brucei*. Bc. Thesis, in English, -39 p., Faculty of Science, University of South Bohemia, České Budějovice, Czech Republic.

Annotation

In this thesis in-situ tagging by parasite transfection, cell transfection followed by Western Blot (WB) and immunofluorescence microscopy methods were applied to the analysis of the endogenous localization of prioritized putatively mitochondrial *Trypanosoma brucei* proteins. Molecular cloning and generation of RNAi constructs were utilized for determination of essentiality.

Declaration

I declare that I am the author of this qualification thesis and that in writing it I have used the sources and literature displayed in the list of used sources only.

Place, date: České Budějovice, 12.05.2021
Student's signature:

Contents

Abbreviations

APRT	Adenine phosphoribosyltransferase
APS	Ammonium persulphate
BSFs	bloodstream forms
CT	C-terminally
CYT	cytoplasm
DAPI	4′,6-Diamidin-2-phenylindol
DNA	Deoxyribonucleic acid
dNTPs	deoxynucleotides
dsRNA	double-stranded RNA
gDNA	genomic DNA
HAT	Human African Trypanosomiasis
HSP70	Anti-Heat Shock Protein 70
IFA	Immunofluorescence assay
kDNA	kinetoplast DNA
min	minutes
MIT	mitochondria
mNG	mNeonGreen
mRNA	messenger RNA
NT	N-terminally
ON	over night
PBS	Phosphate buffered saline
PBS-T	Phosphate buffered saline + tween 20
PCR	Polymerase Chain Reaction
PFs	procyclic forms
PVDF	Polyvinylidene fluoride
RNA	Ribonucleic acid
RNAi	ribonucleic acid interference

RT	room temperature
SDS-PAGE	Sodium Dodecyl Sulphate-Polyacrylamide Gel Electrophoresis
T. b.	*Trypanosoma brucei*
T. brucei	*Trypanosoma brucei*
TAC	Tripartite attachment complex
TEMED	N,N,N',N' Tetramethylethylenediamine
tween20	Polysorbate 20
vPBS	Vorheis' modified PBS
WB	Western Blot
WCL	whole cell lysate
x	times

Acknowledgment

I am extremely grateful to my supervisors Dr. Ignacio Durante and Mgr. Vendula Rašková who guided me throughout the whole project and supported me in any kind of concern.

I also wish to thank Prof. RNDr. Julius Lukeš, CSc. who accepted me in his laboratory and even made it possible for me to continue working on my project during the COVID-19 pandemic.

Further, I would like to thank all members of the Laboratory for helping where necessary and creating a friendly working atmosphere.

Introduction

Trypanosoma brucei is a flagellated protozoan causative agent of Human African Trypanosomiasis (HAT) and *nagana* in cattle, member of the class Kinetoplastea, comprising several other parasites causative of human and zoonotic diseases of superlative sanitary relevance, as American Trypanosomiasis caused by *Trypanosoma cruzi*, and leishmaniases caused by *Leishmania* spp (Barrett et al., 2003). The *T. brucei* subspecies causing Human African Trypanosomiasis are *T. b. gambiense* and *T. b. rhodesiense*, while *T. b. brucei* affects wild and domestic animals. Other species non-pathogenic to humans are *T. congolense*, and the causative agents of durine and surra diseases in camels and horses, *T. b. evansi* and *T .b. equiperdum*, respectively (Brun et al., 2010).

Adapted to diverse environments, dixenous *T. brucei* exhibits a complex life cycle alternating between an insect and mammalian host. In the tse-tse fly brucei bloodstream forms taken from the mammalian host differentiate into dividing midgut procyclic forms and sequentially into migrating epimastigotes and metacyclic forms in the salivary glands that infect the mammal host and differentiate into polymorphic dividing slender and short stumpy forms, taken by the tse-tse fly during a blood meal (Brun et al., 2010).

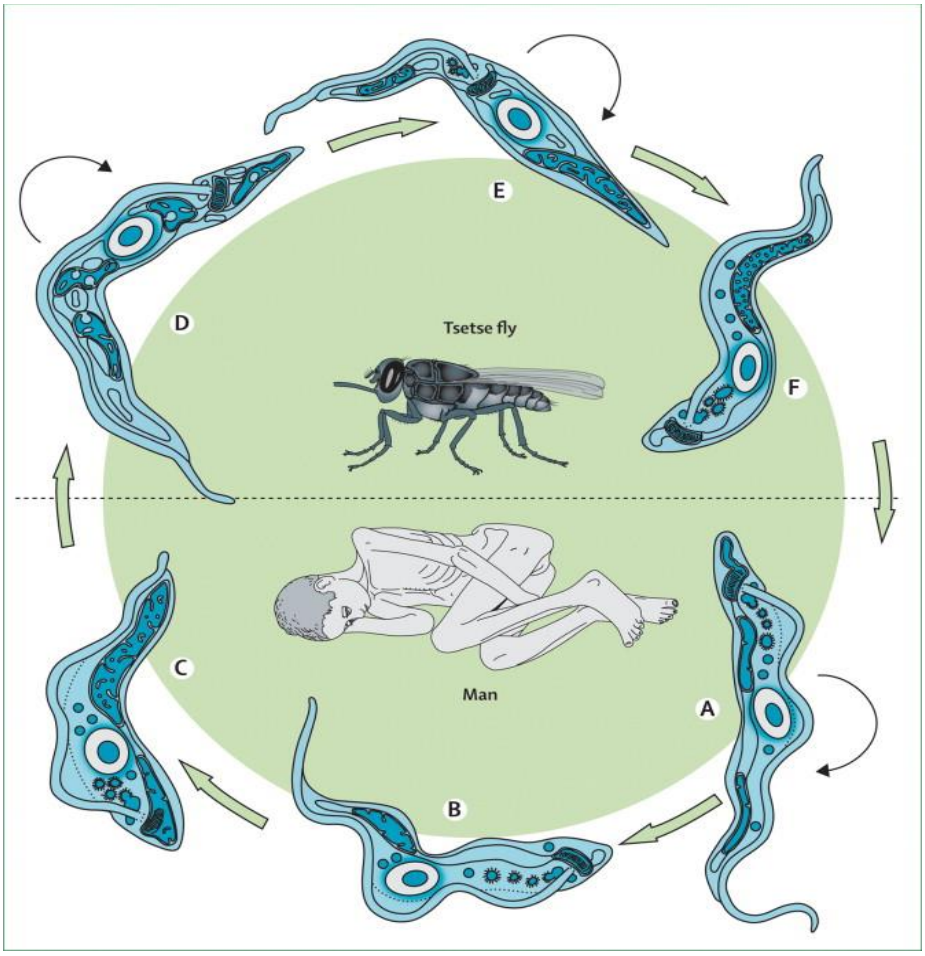

Figure 1. Life cycle of T. brucei. *Dividing long slender (A), intermediate (B) and short stumpy (C) BSFs in the mammalian host and dividing midgut PFs (D), migrating epimastigotes (E), and infective metacyclic trypomastigotes in the tse-tse fly (F). Reference: Brun et al., 2010.*

As well as other trypanosomatids, *T. brucei* is a highly complex cell that amongst other organelles exhibits specialized peroxisome-related membranous glycosomes, where glycolysis is compartmentalized (Parsons, 2004). Glycosomes enzymatic composition is dynamic; ca. 90% of glycosomal enzymes in BSFs are devoted to glycolysis, while PCFs can switch between glycolysis and amino-acid catabolism and TCA cycle as source of ATP, and therefore ca. 50% of glycosomal enzymes are involved in glycolysis (Bauer & Morris, 2017).

A large single mitochondrion composed of ca. 1008 proteins identified with variable degree of confidence (Panigrahi et al., 2009), is a highly dynamic organelle that also suffers extensive remodeling during *T. brucei* life cycle, exhibiting relatively abundant and diminished *cristae* in PCFs and BSFs respectively, partly reflecting the transitions regarding energetic metabolism: from oxidative phosphorylation in PCFs to substrate-level phosphorylation in BSFs (Bílý et al., 2021).

The Tripartite attachment complex (TAC) physically connects the kDNA to the basal body of the flagellum to ensure the proper segregation of the mitochondrial genome during cell division. Depletion of these TAC components were associated with defects in growth either in procyclics (PCF) or bloodstream forms (BSF) and/or kDNA segregation during cell division and targeting to the TAC was attributable to either N- or C-terminal import signals (Schneider & Ochsenreiter, 2018).

Due to their medical and economical relevance, the genomes of *T. brucei* as well as related trypanosomatids have been extensively sequenced and are available in the genome database TriTrypDB, allowing for the characterization of their proteomes in the post-genomic era (Aslett et al., 2009).

Triptag.org was formed to achieve a transformative -resource for enabling sophisticated analysis of conserved eukaryotic and parasite specific cell biology. Protein locations were determined by using mNG fluorescent protein tagging to validate proteomic analyses. Endogenous tagging of protein genes using long-primer PCR to generate the construct got optimized to make it more efficient, scalable, and reproducible. Thus, allowing the investigation of up to 192 PFs cell lines each week and making them available online (Dean et al., 2017).

Preliminary results

Taking advantage of localization data available in the tryptag database (tryptag.org), identification of several candidates that were determined to be mitochondrial and putatively related to TAC structures was performed. Prioritization was carried out based on bibliographic assessment of previous characterization, inspection of micrographs on tryptag database and sequence similarity-based assigned function and/or domains.

As a result, the following candidates were chosen for investigation:

GI[a]	Description[b]	Prosite[c]	Superfamily[d]	NT[e]	CT[f]
Tb927.2.5020	acyl-CoA oxidase, putative	N/A	Acyl-CoA dehydrogenase C-terminal domain-like;Acyl-CoA dehydrogenase NM domain-like	CYT	TAC
Tb927.6.1570	2-hydroxy-3-oxopropionate reductase, putative	N/A	6-phosphogluconate dehydrogenase C-terminal domain-like;NAD(P)-binding Rossmann-fold domains	CYT	TAC
Tb927.8.1440	maoC-like dehydratase, putative	N/A	Thioesterase/thiol ester dehydrase-isomerase	CYT	TAC, CYT
Tb927.8.6970	3-methylcrotonyl-CoA carboxylase alpha subunit, putative	Biotinyl/lipoyl domain profile;ATP-grasp fold profile;Biotin carboxylation domain profile	Single hybrid motif;Rudiment single hybrid motif;PreATP-grasp domain;Glutathione synthetase ATP-binding domain-like	CYT	TAC

Figure 2: The GIs of the final candidates proposed for characterization is shown. [a] : Gene identifier, [b] : as annotated in tritrypdb, [c] : domains annotated in Prosite, [d] : Superfamily annotation, [e] : N-terminal Neongreen tagging, [f] : C-terminal mNG tagging (tryptag). Abbreviations: CYT; cytoplasm, MIT; mitochondrion, K; kinetoplast, TAC; tripartite attachment complex, N.D.; not determined.

The deposited tryptag data (tryptag.org) for the localization of CT and NT mNG tagged proteins was evaluated for every candidate (Fig. 3). Interestingly, a "TAC-like" associated distribution of the fluorescent signal in all CT tagged candidates and cytoplasmic expression of NT-mNG fused constructs was found, suggesting that NT tagging may abolish some NT translocation signal to the TAC. In fact, many other hypothetical proteins not included here displayed the same pattern of behavior and bear putative N-terminal SP signals. CT mNG products were also found to display dual localization, associated in some cases with MIT and CYT compartments in addition to TAC related localization.

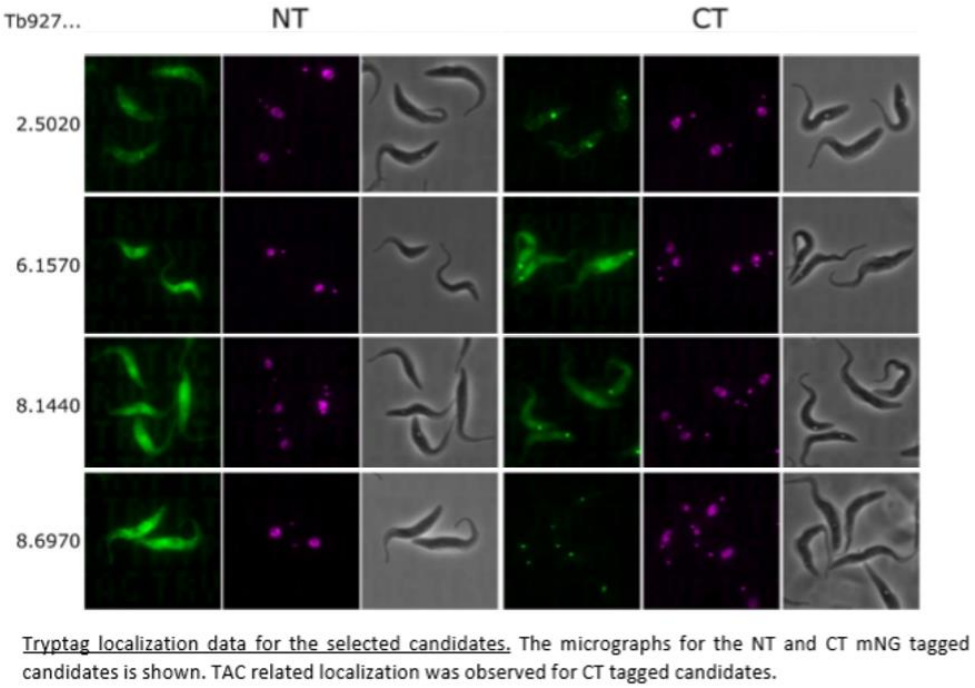

Figure 3: TripTag micrographs corresponding to the prioritized candidates, blue DAPI, green mNG, each indicating punctual localizationin the CT pannel

The dual NT CT localization was prompting to validate whether the selected candidates were indeed TAC related or corresponding to the cytoplasm or mitochondria.

Aim of work

The aim of the project was to determine the subcellular localization of the prioritized *T. brucei* genes Tb927.2.5020 (acyl-CoA oxidase), Tb927.6.1570 (2-hydroxy-3-oxopropionate reductase), Tb927.8.1440 (maoC-like dehydratase), and Tb927.8.6970 (3-methylcrotonyl-CoA carboxylase alpha subunit) by in situ-tagging with CT V5-tagged versions of the proteins using a pPOT based *in situ* tagging strategy. Over these obtained cell lines fine localization assessment by IFA and further WB analysis over CYT/MIT subcellular fractionations were performed. Additionally, constructs for monitoring the effects of the ablation/knock down of the expression of the candidates' products by RNAi were generated by a pTrypson-based strategy, and the growth phenotype of Tb.927.8.1440 was evaluated.

Materials and Methods

Polymerase Chain Reaction

PCR reactions were performed for amplifying inserts and stuffer as well as the backbones for pTrypson Gibson assembly cloning.

During a typical PCR, template DNA is mixed with dNTPs, a DNA polymerase and primers. Primers are short segments of complementary DNA that base-pair with the template DNA, upstream of the region of interest, and serve as recruitment sites for the polymerase. PCR involves a series of temperature cycles that are controlled automatically by the use of a thermocycler that precisely controls both the reaction temperature and the duration of each temperature step, ensuring efficient amplification (Kadri, 2019).

A PCR reaction is generally performed based on 5 steps.

i. Initialization step to heat activate DNA polymerase
ii. Denaturation step to break hydrogen bonds between double strands of genetic material
iii. Annealing step to allow primers to attach to single stranded genetic fragments
iv. Elongation step were new stands are being synthesized
v. Final elongation to check that all strands are fully extended

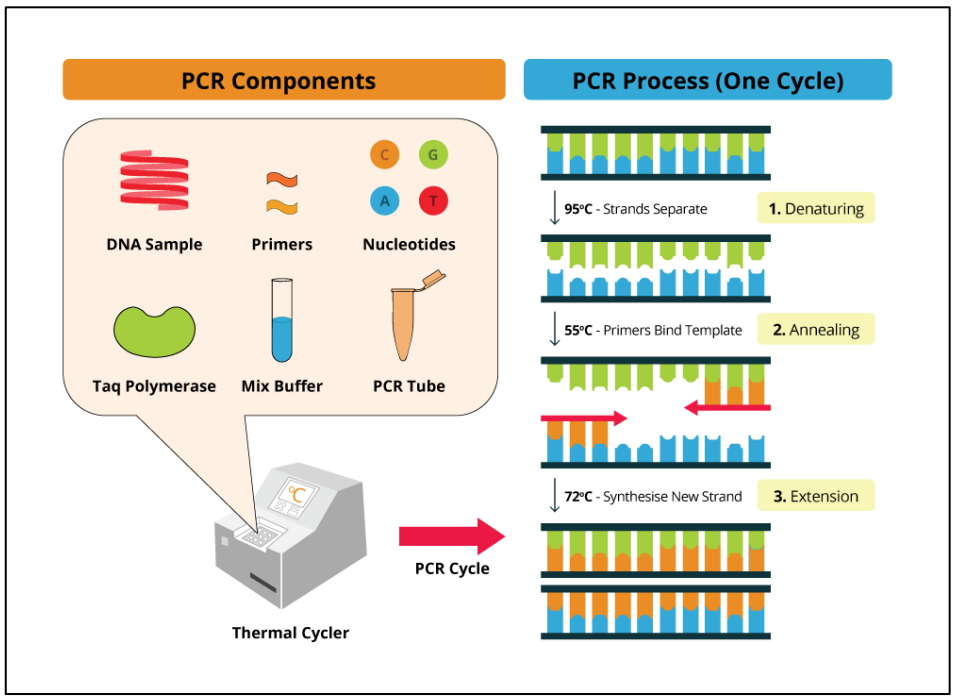

Figure 4: PCR scheme

PCR can be used to rapidly generate DNA fragments for cloning, provided that a suitable source of template DNA exists, and sufficient sequence information is known to permit design of primers specific for the desired amplicon. Unlike traditional cloning, PCR offers the ability to readily clone DNA fragments that may be of low abundance in a complex sample such as genomic DNA, or cDNAs that correspond to rare mRNA transcripts. PCR products can be digested and ligated by traditional means, ligated directly, or used in ligation independent cloning or seamless cloning applications, such as Gibson Assembly, which was done during this project (Kadri, 2019).

Long primer PCR and tagging

Endogenous tagging was performed for cell localization of the selected proteins, as described in the TrypTag database. 80 nucleotides are required for homologous recombination within the organism (Dean et al., 2015). These are needed for genomic recombination of the PCR products. Primer is only partially homologous to the PCR template and the rest is determined to be the overhang coding for the target gene locus. Several plasmids named pPOT were produced to establish a conspicuous long primer PCR tagging method achieving tagging of the genes at both C and N termini or within the gene itself to generate deletion mutations to analyze properties of the several protein domains (Dean et al., 2015).

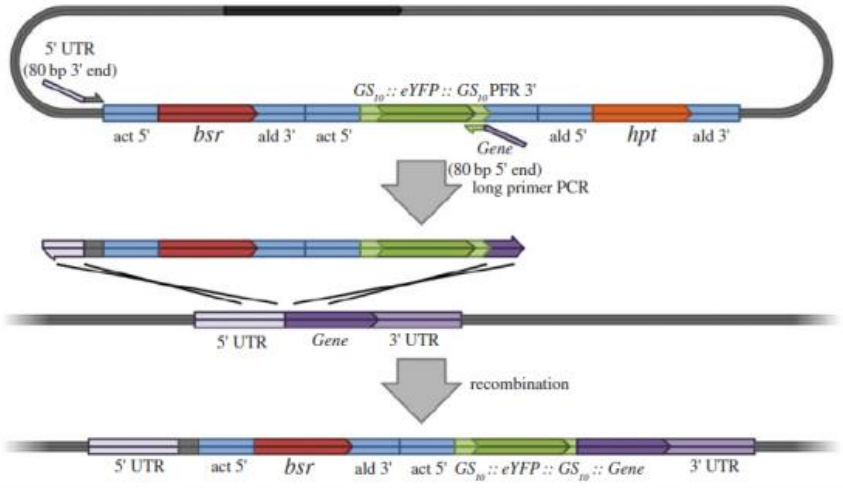

Figure 5: Example of long primer PCR tagging N-terminal end using pPOTv4, adapted from (Dean et al., 2015)

For creating the required vectors for tagging, each corresponding primer pair was mixed with 25 µL Q5 hotstart, 23 µL water and 0,5 µL of pPOT V5 vector available in our laboratory.

In a similar way a PCR reaction mix for the primer pairs for RNAi was set up. Therefor the primer pairs got mixed with 25 µL Q5 hotstart, 23 µL water but instead of a pPOT V5 vector 1 µL genomic DNA was added per reaction.

Samples were further processed in a thermal cycler and checked by agarose gel electrophoresis.

Gibson Assembly

Gibson assembly constitutes a robust exonuclease-based method to assemble DNA seamlessly and in the correct order. The reaction is carried out under isothermal conditions by making use of three enzymatic activities: 5´ exonuclease, the 3´ extension activity of a DNA polymerase and DNA ligase activity. The 5´ exonuclease activity chews back the 5´ end sequences and reveals the complementary sequence for annealing. The polymerase activity then packs the gaps on the annealed regions. A DNA ligase then seals the nick and covalently joins the DNA fragments together (Gibson et al., 2009).

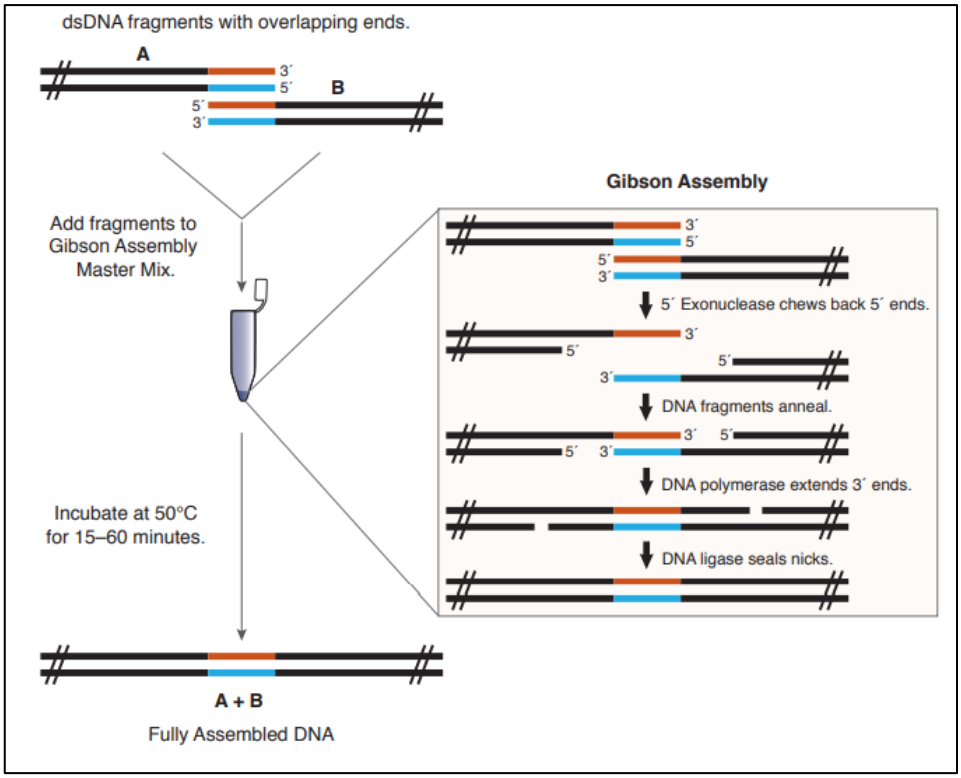

Figure 6 (From: https://www.addgene.org/protocols/gibson-assembly/)

The reaction mix (see Appendix) based on which the Gibson assembly was performed then got combined with produced PCR products/fragments and incubated at 50°C in a thermal cycler for 1 hour. Afterwards samples were stored on ice for subsequent transformation.

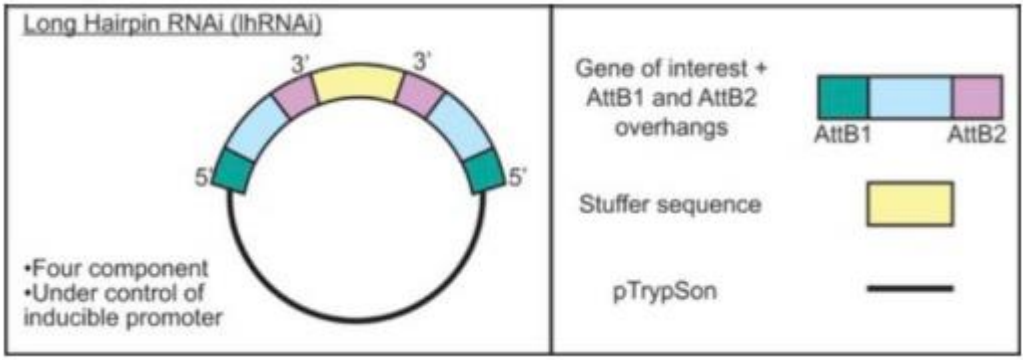

Figure 7: Schematic representation of TbPLKpTrypSon plasmid for lhRNAi, adapted from (McAllaster et al., 2016)

The plasmid used for inserting lhRNAi was generated by Gibson assembly permitting a fast connection of several overlapping DNA fragments in an individual reaction. This is being done in 3 steps. Beginning with Exonuclease T5, which is chewing back linear DNA in 5' to 3' direction without affecting closed circular molecules, allowing complementary overlapping chains to anneal together. Created gaps are then being closed by a specific polymerase, and nicks are being fixed by DNA ligase (Gibson et al., 2009).

Transformation

Approximately 3 µL of each obtained Gibson assembly product were mixed with 50 µL XL-1 Blue bacteria followed by an incubation on ice for 30 min. Bacteria were subjected to heat shock at 42°C 40 seconds and again placed on ice for 5 min. Bacteria were incubated at 37°C for an hour into 1 mL of LB media. Samples were transferred into new Eppendorf tubes and centrifuged at 3000 rpm for 10 min. Samples were then plated in ampicillin Petri dishes and incubated ON at 37°C. Colonies were screened for presence of inserts and spacer in the correct orientation by colony PCR.

Colony PCR

Colony PCR is a convenient high-throughput method for controlling the presence or absence of insert DNA in plasmid constructs. Individual transformants can either be lysed in water with a short heating step or added directly to the PCR reaction and lysed during the initial heating step. This initial heating step causes the release of the plasmid DNA from the cell, so it can serve as template for the amplification reaction. Primers designed to specifically target the insert DNA can be used to determine if the construct contains the DNA fragment of interest. Alternatively, primers targeting vector DNA flanking the insert can be used to determine if the insert is the correct molecular size. Insert specific primers can provide information on both the specificity and size of the insert DNA while the use of vector specific primers allows screening of multiple constructs simultaneously. Colony PCR can also be used to determine insert orientation. PCR amplification of the plasmid using an insert specific primer paired with a vector specific primer can be designed to produce an amplicon of a specific size only if the insert is in the correct orientation. In all experimental designs, presence or absence of a PCR amplicon and size of the product are determined by electrophoresis alongside a DNA size marker on an agarose gel (Azevedo et al., 2017).

Agarose gel electrophoresis

1% w/V gels were made by mixing 0.8 g of solid Agarose with 80mL of 1x TAE buffer and 0,5 μg/mL final concentration of ethidium bromide. After gelation samples were mixed with loading buffer and loaded into the gel. Electrophoresis was performed at 100-110 V for around an hour. Visualization was performed by UV illumination under ChemiDoc. This was done to check if PCR reactions were successful as in agarose gel electrophoresis different nucleotide fragments are separated based on their length, as they travel throughout the gel in the direction of the cathode due to their negative charged phosphate backbones.

Parasite cultures

All obtained cell lines were grown in an incubator at 27°C in T-25 culture flasks. Approximately every 48h a dilution of the cultures to a density of 10^6 to $2x10^7$ cells per mL was performed with SDM-79 mixed with the appropriate antibiotic.

Transfection and Selection

For transfection, SMOX cells were harvested by spinning them down at 1300 x rcf at 4°C for 10 min. After centrifugation, the cell pellet was resuspended in 80 µL of Human T-cell nucleofector and 20 µL of Supplement 1 combined in a total volume of 100 µl. Resuspended cells were mixed with 10-12 µg of NotI linearized DNA, placed into a cuvette and electroporated in AMAXA machine under program: X-014. After transfection, cells were placed into culture T-25 flaks containing 6 ml SDM-79 media and incubated for 16-18 hours or ON at 27°C.

After this incubation, 6 mL of SDM-79 media containing either hygromycin or phleomycin antibiotic at 2x concentration was added to the flaks. The mixture then got transferred a 24 well plate with serial dilutions and a final volume of 1,5 mL/well. 5 mL of fresh media plus antibiotic was added to the remaining cells in the flasks. 50 µg/ml hygromycin was used for tagging cells, whereas phleomycin was used to select RNAi constructs. SMOX cell lines were used as growth control, treated with the same antibiotic as abovementioned cell lines. Resistant clones emerged after approximately 10-14 days.

Immunofluorescence assay

An immunofluorescence experiment is based specific antibodies binding to the protein of interest and fluorescent dyes that are coupled to these immune complexes in order to visualize the protein of interest using microscopy.

After harvesting approximately 10^6 cells, a 2x washing step with 1 mL vPBS (PBS supplemented with 10mM glucose and 46mM sucrose, pH 7.6) -was performed. Cells were resuspended in 200-400 µL vPBS were added and 20 µL of the cell suspension got transferred to a microscopic slide. After an incubation period of 10 min, the remaining liquid with non-attached cells got replaced with 4% paraformaldehyde and cells were fixed for another 15 min at RT. After fixation, cells were permeabilized with 0.1% Triton X-100 in PBS (TX-100) for 15 min, followed by blocking for 1h in 1% BSA in PBS supplement with 0.033% TX-100 (washing buffer) and same concentration of TX-100 was also used for washing steps. Monoclonal alpha-mtHsp70 antibody was used as mitochondrial marker. Rabbit alpha-V5 was used for V5 tagged proteins. Incubation was done ON with the corresponding antibodies at 1:1000 dilution.

The next day 3x washing steps in washing buffer were performed and incubation in secondary antibodies (goat α-rabbit Alexa Fluor 488 and goat α-mouse Alexa Fluor 555) was carried out. To eliminate unspecific binding of the antibodies 3x washing steps in washing buffer were completed and DNA got stained with DAPI included in ProLong1 Gold antifade reagent mounting solution. Observation was performed with a Zeiss microscope Axioplan 2 equipped with an Olympus DP73 digital camera. Images were processed by ImageJ.

Sample Preparation for SDS-PAGE and Western Blot

Total lysate preparation:

Cells with a concentration of approximately $1*10^7$ cells/mL were harvested by spinning them down at 900 xg for 3 min. Afterwards pellets then were washed twice in PBS and lysis buffer was added. Cells then were heated at 95°C for 5 min and loaded into the gel.

Cytoplasm-mitochondria fractionation:

Cells (around 4mL of cell line media) were harvested 1000 xg at 4°C for 10min. Supernatant of sample was discarded, cell pellets were washed twice in 1x PBS and resuspended in 500 µL ice-cold lysis buffer. 100 µL out of the total 500 µL suspension mix were transferred to a separate tube and labeled as WCL. The remaining 400 µL were mixed with 16 µL of digitonin to obtain a final concentration of 0.4mg/mL, vortexed and incubated at RT for 5 min. Tubes then were spinned down @14000g at RT for 2 min. Obtained supernatant got stored and labeled as CYT. Remaining cell pellets were washed in lysis buffer and afterwards resuspended in fresh 400 µL of lysis buffer and 4 µL Triton -X100 was added to obtain a final concentration of 0.1%. Samples then were incubated on ice for 5 min and labeled as MITO fraction.

Obtained cell fractionations were used to determine subcellular localization by further WB analysis.

SDS-PAGE

15 µL of either total lysate or CYT-MITO fractions samples were mixed with 5 µL of loading buffer and cracked by heating 5 min at 95°C.

Gels were made (components and concentrations in appendix), SDS-PAGE machine was set up and filled with running buffer (appendix), followed by loading the samples into the gel.

For separation of proteins a voltage of 110V was applied for approximately 90 min.

For validation of the achieved expressions, SDS-PAGE and Western Blot experiments were performed. SDS-PAGE allows separating proteins by using the properties of solubilization in anionic detergents (Rajput & Sharma, 2011). These negative charges are being created as in the presence of SDS secondary and tertiary protein structures are being broken up.

When an electric field is applied, heavier proteins will migrate slower, while lighter will migrate faster towards the cathode, and thus separation is obtained in a denaturing SDS-PAGE. The polyacrylamide gel is produced out of a running and stacking gel, each with different concentrations of polyacrylamide and pH values (Rajput & Sharma, 2011).

Western Blot

Western blot analysis was performed by transferring the separated protein from the SDS-PAGE onto a polyvinylidene difluoride membrane (PVDM) followed by immunolabeling. This was obtained due to a primary antibody binding to a certain epitope of the protein of interest (Yang & Mahmood, 2012). A secondary antibody then is utilized which attaches to the prior used one. Upon applying ECL substrate chemiluminescent reaction will be enhanced emitting detectable light.

For Western Blot a blotting, a blocking milk (5% m/V milk in PBS 0,05% V/V tween20), and a PBS tween20 0,05% V/V solution were prepared.

Transference of SDS-PAGE separated to methanol activated PVDF membranes was performed by placing sponges and Filter Papers in blotting buffer, packing the membrane and SDS-PAGE gel as shown in Figure 7.

Membranes were blotted at 110 V for around 1.10h-1.15h, after which a blocking step for one hour in blocking milk was followed before incubating in blocking milk with primary antibody in the appropriate concentration over night. The next day membrane got washed 5x in PBS with tween20 for 5 min each, followed by incubation in blocking milk and secondary antibody in the appropriate concentration for an hour. After incubating in secondary antibody membrane got washed again 5x in PBS for 5 min to get rid of unspecific bound substrates.

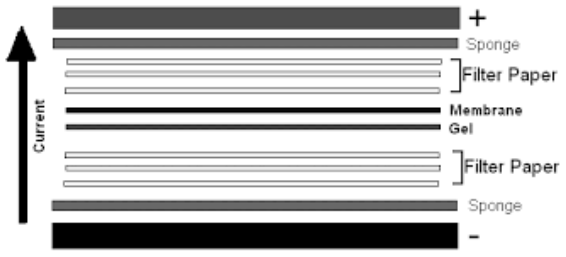

Figure 8: Western Blot arrangement

RNA interference

RNAi or RNA-Silencing is a natural biological mechanism within cells of many eukaryotes, which is used to specifically switch off genes, and normally directed against RNA viruses. It is based on interactions of short pieces of RNA fragments with the mRNA. Due to cleaving of the dsRNA by nuclease dicer into non-coding RNA molecules, antisense strands can be embodied into RISC (RNA-induced slicing complex), which is then directed to the complementary mRNA strand. This strand, due to the enzyme Argonaute 2 in RISC, is then being disjointed and cannot be translated into a protein any longer, resulting in its loss of function.

RNAi is exploited as a molecular method utilized to determine gene function within *T. brucei* (McAllaster et al., 2016). In this concern, long hairpin RNAi (lhRNAi) experiments were selected to produce constructs and determine their loss-of-function. This was performed with a pTrypSon plasmid backbone containing required sequences for generating RNAi hairpins with stuffer connecting oppositely oriented target regions. Followed, a double-stranded DNA is achieved as a hairpin structure is obtained after expression under tetracycline induction (McAllaster et al., 2016).

Growth Curves

Four distinct phases of growth can be determined within a curve.

The lag phase shows slow growth or lack of growth due to physiological adaptation of cells to culture conditions or dilution of exoenzymes due to initial low cell densities. In the next phase, the logarithmic or exponential phase optimal growth rates, during which cell numbers double at discrete time intervals known as the mean generation time are visible. In the Stationary phase growth (cell division) and death of cells counterbalance each other resulting in no net increase in cell numbers. The reduced growth rate is usually due to a lack of nutrients and/or a buildup of toxic waste constituents. In the death phase is followed in which death rate exceeds growth rate resulting in a net loss of viable cells (Maier et al., 2000).

Standard growth curves were performed in Tb.927.8.1440 RNAi transfected line by measuring the cell concentration each day in an automatic cell counter and diluting them every time in media with or without 1 µg/ml tetracycline.

Results

Endogenous gene tagging and pTrypson RNAi construct generation

To generate PCRs for tagging and pTrypson RNAi constructs, two distinct PCR reactions were performed.

PCR tagging products as well as inserts for cloning into pTrypson for all four candidates were obtained after performing the PCR reactions. For insert generation PCR over gDNA from *T. brucei* was performed. As template for the tagging PCR pPOT vectors were used.

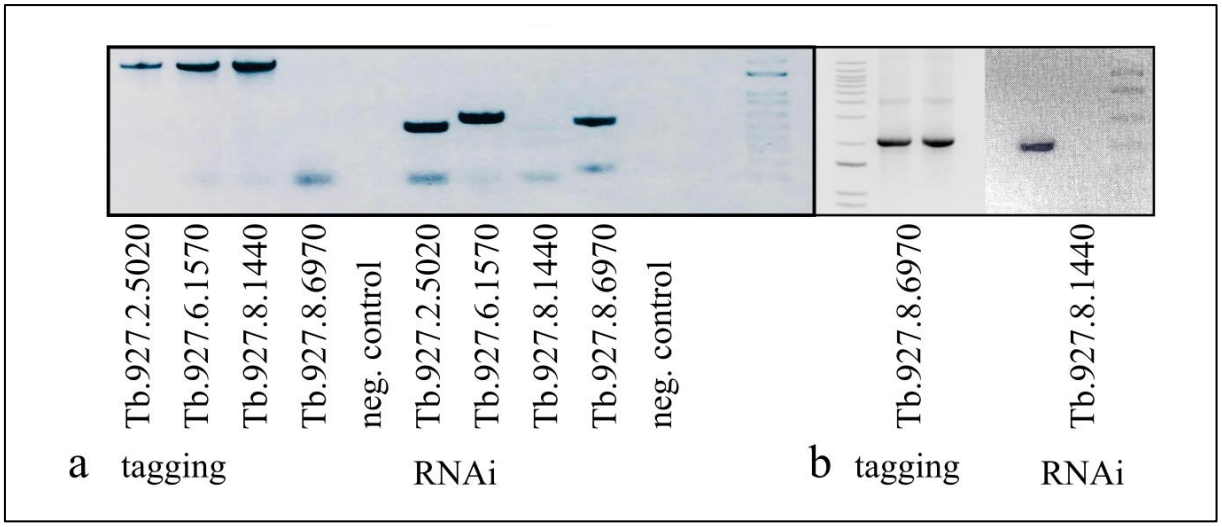

Figure 9: gDNA and tagging vector PCR results, a) first round PCRs, b) second round PCRs, each lines corresponds to one PCR reaction of a prioritized candidate indicated by GI, left: tagging PCR results, right: RNAi insert gen. Negative control did no include template

Gibson assembly cloning by PCR over gDNA was performed to insert the genes of interest into pTrypson backbone together with the stuffer followed by further transformation of XL-1 Blue bacteria with ligations. Afterwards, diagnostic colony PCR was carried out.

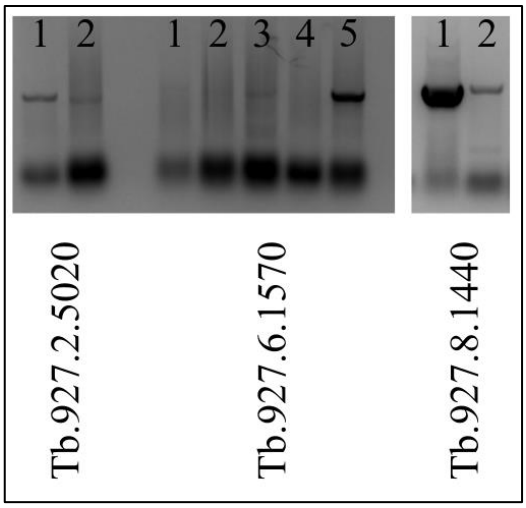

Figure 10: Colony PCR results for Tb.927.2.5020, Tb.927.6.1570 and Tb.927.8.1440, PCR was performed with primers gRNAi forward and gRNAi reverse (sequences in appendix)

Suitable colonies for Tb.927.2.5020 (colony 1), Tb.927.6.1570 (colony 5) and Tb.927.8.1440 (colonies 1 and 2) were cultivated and sended for sequencing. Protein Tb.927.8.1440 then was transfected in order to obtain T. brucei procyclic RNAi stain depicted below.

Based on the obtained cell cultures further investigation of the subcellular localization of the proteins with WB was carried out.

Tagging and subcellular localization analysis of prioritized candidates

Transfections were performed over SMOX procyclics with products of long primer PCRs.

For all four proteins the perfomed Westen Blot indicated that the genes were succesfully introduced into the cell lines. In each cell line the protein could be detected within the whole cell lysate.

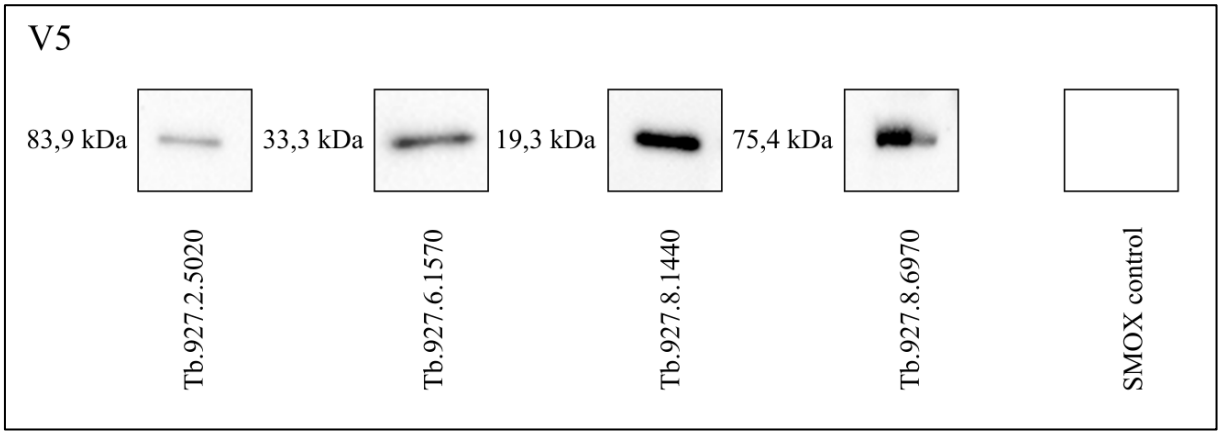

Figure 11: whole cell lysate V5 WB results for Tb.927.2.5020, Tb.927.6.1570, Tb.927.8.1440, Tb.927.8.6970 and SMOX control

To determine the subcellular localization of the proteins within the cell IFA over transfected procyclics was performed (Fig. 13).

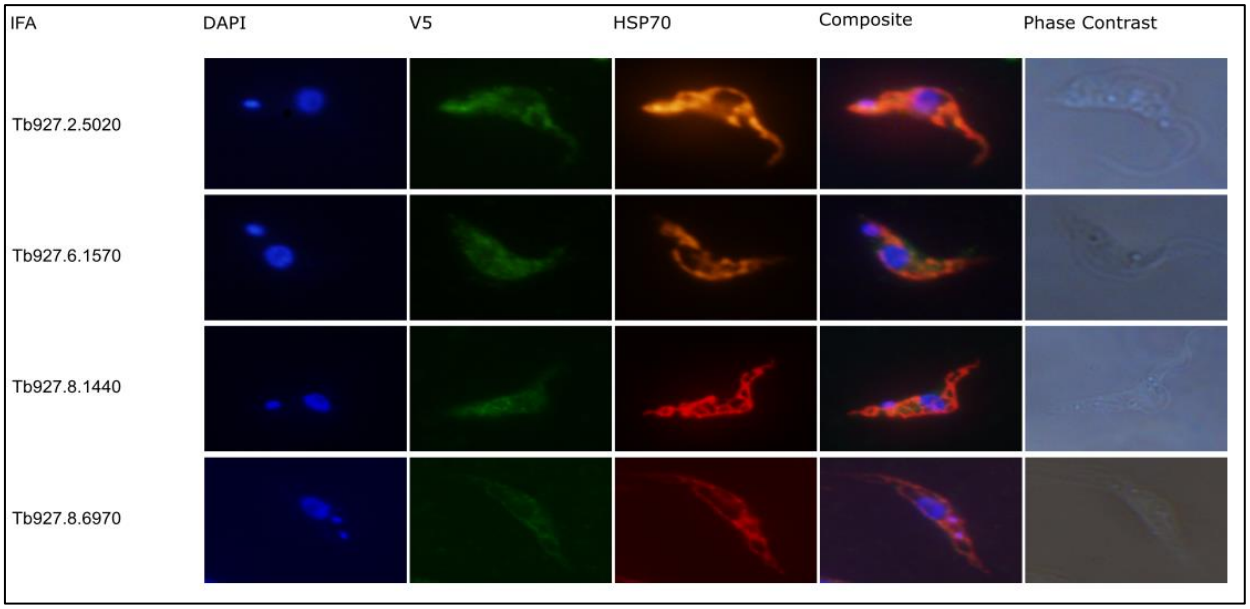

Figure 12: Immunofluorescence assay showing V5-tagged candidates (in green), compared to the HSP70 (in red). DAPI is shown in blue. The composite shows the merge of the three channels accompanied by their phase contrast indicating normal cell growth.

For all protein cells the V5 tag showed in green has a very low signal strength in comparison to the HSP70 signal being much stronger. Overlaps with mitochondrial HSP70 only for Tb.927.2.5020 and Tb.927.8.6970 could be observed while Tb.927.6.1570 and Tb.927.8.1440 appeared to display signal located throughout the cell body, therefore compatible with cytoplasmic staining.

For Tb.927.2.5020 and Tb.927.8.6970 the signals of the V5 tag and HSP70 are overlapping. A normal IFA result, under these given circumstances, would give rise to a yellow signal in the composite for our proteins, which is not abundant in our case. This is probably due to the low signal intensity obtained for our V5 tags. Thus, mitochondrial subcellular localization of Tb.927.2.5020 and Tb.927.8.6970 was observed.

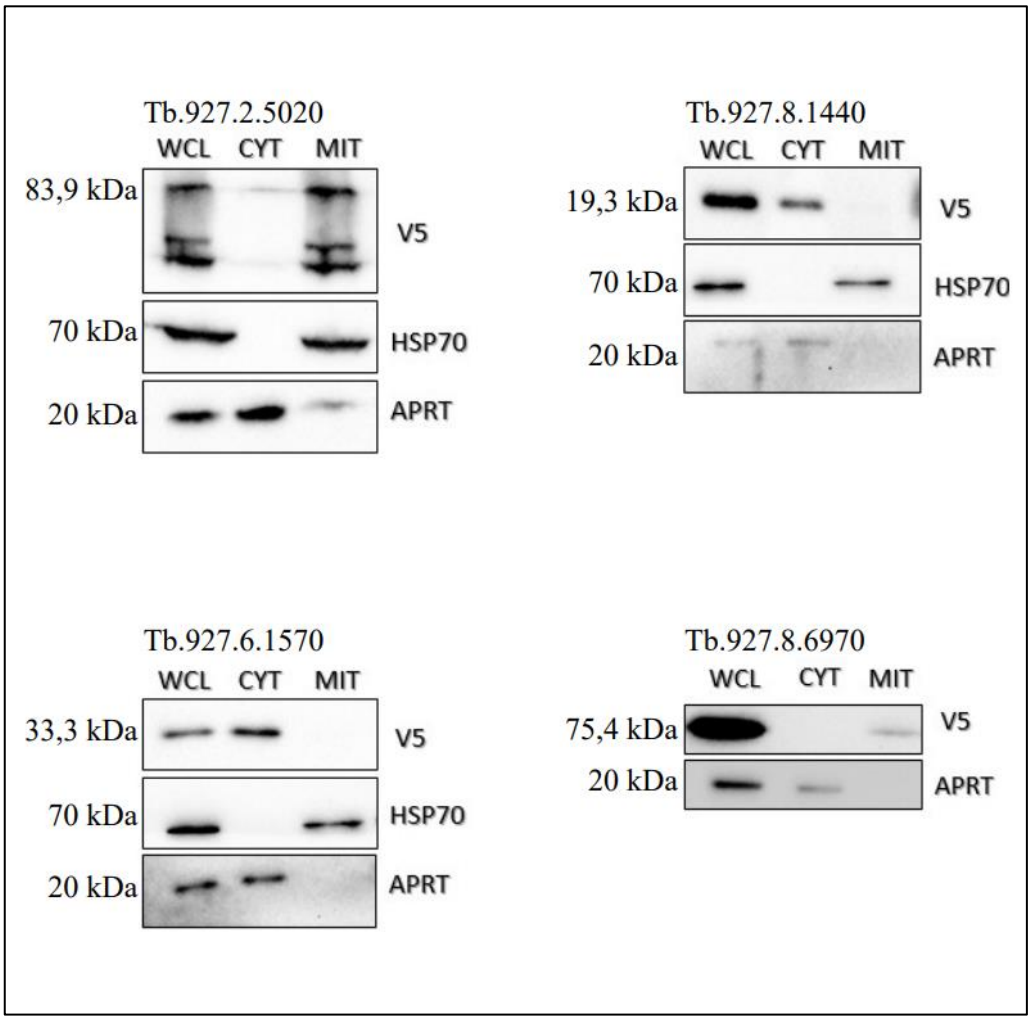

Figure 13: cellular fractionation WB results of Tb.927.2.5020, Tb.927.6.1570, Tb.927.8.1440 and Tb.927.8.6970, WCL: whole cell lysate, MIT: mitochondrial fractionation, CYT: cytoplasmic fractionation, HSP70: mitochondrial control, APRT: cytoplasmic control

The aim of performing WB over cellular fractionation for Tb.927.2.5020, Tb.927.6.1570, Tb.927.8.1440 and Tb.927.8.6970 was to obtain another line of evidence to assess their localizations. As controls for mitochondrial and cytoplasmic localization HSP70 and APRT antibodies were used, respectively.

Based on the Western Blot results it can be concluded that proteins Tb.927.2.5020 and Tb.8.6970 have a mitochondrial subcellular localization. Tb.927.6.1570 and Tb.927.8.1440 instead seem to be cytoplasmic.

As in the IFA composites of Tb.927.6.1570 and Tb.927.8.1440 the green signal of the V5 tag is still visible and not completely overlapping with the red signal of HSP70, a cytoplasmic subcellular localization can be expected, thus WB results are in good agreement with results obtained by IFA for Tb.927.6.1570 and Tb.927.8.1440.

Furthermore as for Tb.927.2.5020 and Tb.927.8.6970 the signals of the V5 tag and HSP70 are overlapping in IFA investigations and obtained cellular fractionation WB results for Tb.927.2.5020 and Tb.927.8.6970 are as well indicating a mitochondrial subcellular localization, obtained results are also in good agreement to each other.

RNAi analysis of Tb.927.8.1440

We analyzed the effects of RNAi ablation for Tb.927.8.1440. Based on the obtained RNAi cell line a growth curve was carried out (Fig. 15). Cells were stably transfected with the RNAi construct of Tb.927.8.1440 in order to assess the essentiality of the gene product.

No effects on the growth of *T. brucei*, due to ablation of Tb.927.8.1440 could not be observed.

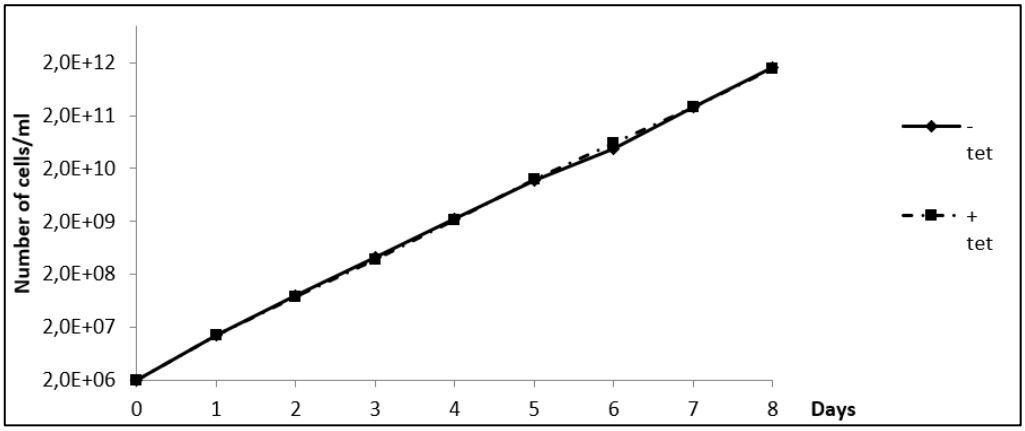

Figure 14: growth curve of RNAi construct from Tb.927.8.1440, standard growth curve, The number of cells per mL is represented in an non induced (-)/induced (+) form with tetracycline over a time range from 9 days (day 0: start, day 8: end) Almost no difference between the induced and non induced form could be observed.

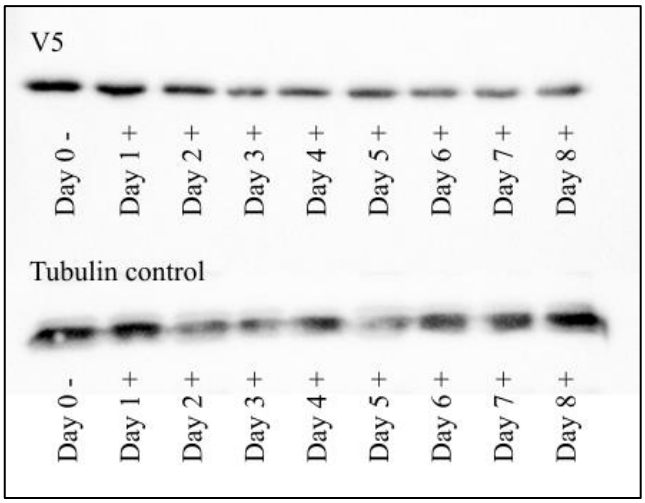

Figure 16: V5 and Tubulin WB results for performed growth curve of Tb.927.8.1440 RNAi construct. Lines correspond to day 0-8, - indicating non induced with tetracycline, + indicating induced with tetracycline. Tubulin control serving as a loading control of samples.

As it is shown in the WB performed to check downregulation of Tb.927.8.1440 (Figure 16) only a very low decrease of the protein expression could be observed over the time range of 8 days of RNAi induction with tetracycline, which is in good correlation with the lack of growth phenotype.

Discussion

To examine the dual localization findings of the TrypTag project regarding the proteins Tb.927.2.5020 (acyl-CoA oxidase), Tb.927.6.1570 (2-hydroxy-3-oxopropionate reductase), Tb.927.8.1440 (maoC-like dehydratase) and Tb.927.8.6970 (3-methylcrotonyl-CoA carboxylase) immunofluorescence microscopy as well as WB with crude cellular fractionations over appropriate controls of the cell lines were carried out.

In contrast to that performed in the TrypTag project, selected proteins were only tagged CT instead of at both termini. Also, mNG, a bulky reporter protein was exchanged by the smaller V5 tag, in order to prevent possible artifactual mis-localization.

CT tagging was preferred over NT due to possible interfering with targeting signal peptides located at the NT and eventually generating wrong localization results.

Differently than stated by the TrypTag project mitochondrial not TAC related subcellular localizations for acyl-CoA oxidase and 3-methylcrotonyl-CoA carboxylase were detected when tagged CT by V5. For the proteins 2-hydroxy-3-oxopropionate reductase and maoC-like dehydratase a cytoplasmic localization was observed, however no point localization by V5 tag could be proven and thus, no TAC related localization was verified.

Our obtained results could be related to other previously performed proteomic analysis of *T. brucei* and *T. cruzi*, a related trypanosmatid, addressing the subcellular localizations for each of the selected proteins and its orthologs.

All four were shown to be detected in *T. brucei* mitochondrial proteome (Zíková et al., 2017). This would be in accordance to out obtained results for acyl-CoA oxidase and 3-methylcrotonyl-CoA carboxylase, which thus seem to be mitochondrial but not for 2-hydroxy-3-oxopropionate reductase and maoC-like dehydratase.

Investigation of possible glycosomal relationships had been carried out based on a prior research project, which tagged glycosomes and performed stable isotope labeling in cell culture (SILAC), such that in antiepitope pull-out experiments a distinguishment between genuine glycosomal components and contaminants according to peptide isotopic signatures could be made (Güther at al., 2014).

For 2-hydroxy-3-oxopropionate reductase and maoC-like dehydratase a possible glycosomal relationship could be reported based on these experiments (Güther at al., 2014). Thus 2-hydroxy-3-oxopropionate reductase and maoC-like dehydratase could eventually as well exhibit a glycosomal subcellular localization.

It was shown that under low-glucose conditions, mis-localization of glycosomal matrix proteins is more tolerated, and matrix proteins can be detected in the cytoplasm prior to import into the glycosome (Bauer & Morris, 2017).

Thus further investigations towards the subcellular localization of 2-hydroxy-3-oxopropionate reductase and maoC-like dehydratase should be carried out to analyze their true localization, as only one ortholog in *T. cruzi* could be found for 2-hydroxy-3-oxopropionate eventually indicating an additional glycosomal relation (Acosta et al., 2019).

Further research perspectives towards a possible glycosomal relation could include performing experiments under distinct glucose levels and utilizing different digitonin fractions with appropriate glycosomal markers.

Conclusion/Summary

The main goal of this thesis was to localize genes Tb.927.2.5020, Tb.927.6.1570 , Tb.927.8.1440 and Tb.927.8.6970 in procyclic form Trypanosoma brucei at the C-terminus, and then use immunofluorescence microscopy and cellular fractionation techniques for its localization. Tb.927.2.5020, Tb.927.6.1570 , Tb.927.8.1440 and Tb.927.8.6970 were previously localized in the cytoplasm by imaging using mNeonGreen in the TrypTag project. To confirm their findings regarding these proteins, immunofluorescence microscopy was performed using markers such as V5 and HSP70.

There was no colocalization between Tb.927.6.1570 and Tb.927.8.1440 to the TAC region in C-terminally V5-tagged cell lines, the same was observed for the signal of HSP70 for these two proteins. Since this was the initial report of TrypTag for Tb.927.6.1570 and Tb.927.8.1440, it would suggest a possible artefact in the result for these particular proteins. For Tb.927.2.5020 and Tb.927.8.6970, in contemporary to the results from TrypTag, overlapping HSP70 signals in IFA were observed. A relation to the TAC region in C-terminally V5 cell lines could as well not be proven. These findings suggest that Tb.927.2.5020 and Tb.927.8.6970 could indeed be bound to or associated to the mitochondrion.

Knockdown studies of Tb.927.8.1440 were performed using long hairpin RNAi. The V5 tagged Tb.927.8.1440 RNAi cell line showed none or a small decrease of the protein observed by WB during the induction of RNAi with tetracycline. This was in agreement with the obtained growth curve where no specific growth phenotype could be assessed. Therefore, no clear prediction of the essentiality of this protein within the cell could be made.

Appendix

Primer sequences

Tb927.2.5020	TAG	AAGAGAAGATGGAGGAATCAAGGGAAGATTTTGATCTTTTCCATGGGCTAGCGGGCAAACAGTCCTTTGCACAAGAGAAAGGTTCTGGTAGTGGTTCC	acyl-CoA oxidase, putative
Tb927.2.5020		CAGGGGATACCAAATTTTCACACGAGTGCGCACTGAAAAAAGAAAAAGAAAGAATCAAGCGATTGAAGTAGTTGAATGCACCAATTTGAGAGACCTGTGC	acyl-CoA oxidase, putative
Tb927.6.1570		GCGAAGGTGATTTGGACAACTCTGCTATCATTGGCGTGTTAGAGCGCATGGCCAACTGCAAGATTAAGGAGACCAAGCCAGGTTCTGGTAGTGGTTCC	2-hydroxy-3-oxopropionate reductase, putative
Tb927.6.1570		AAAAATGCCCATGTGCGTGTGCGTATGCGTTTGTTGAAAACGACAAACAGTTACCGATCTGAGGATGATTGGGGAGATTGCCAATTTGAGAGACCTGTGC	2-hydroxy-3-oxopropionate reductase, putative
Tb927.8.1440		GTATCGAAGGCACTGCGGTGGGCATGAACAAGACAGTTACCTTTGAAGGTGAGAGCGAGTGGAATGTGCCCCGTGTCGAGGGTTCTGGTAGTGGTTCC	maoC-like dehydratase, putative
Tb927.8.1440		CCCCCAACGCTCCCAAAACAAGAAGACGAGAAAATGCAAAACGGTACGGCACAACCTCCTTTCTTCGTTAACGTCAAACGCCAATTTGAGAGACCTGTGC	maoC-like dehydratase, putative
Tb927.8.6970		GAGAGGTGAAGTTTTGCGTTCATGCAGATGGCATAGTCGGAGGAAGCACTTTACTTGCCCATATTGCCTCTGCTGCAGTTGGTTCTGGTAGTGGTTCC	3-methylcrotonyl-CoA carboxylase alpha subunit, putative
Tb927.8.6970		TGTGGATGGCGCTGCACAGGGCAAGGAAAACAAAACCGGTTGAAGGCCCCTACAACTTGCAGTCGAAGCGCCTCTAAGCTCCAATTTGAGAGACCTGTGC	3-methylcrotonyl-CoA carboxylase alpha subunit, putative
Tb927.2.5020	RNAi	ACAAGTTTGTACAAAAAAGCAGGCTAAGCTTGCGAGGCCGATTAATGGAGA	acyl-CoA oxidase, putative
Tb927.2.5020		ACCACTTTGTACAAGAAAGCTGGGTCTCGAGGAAGTACAGGGTTCCGGCAA	acyl-CoA oxidase, putative
Tb927.6.1570		ACAAGTTTGTACAAAAAAGCAGGCTAAGCTTCGTCGATGTCGTCTTCACCA	2-hydroxy-3-oxopropionate reductase, putative
Tb927.6.1570		ACCACTTTGTACAAGAAAGCTGGGTCTCGAGCCTCGCGGAATCCATTACGA	2-hydroxy-3-oxopropionate reductase, putative
Tb927.8.1440		ACAAGTTTGTACAAAAAAGCAGGCTAAGCTTCGGATCGGTGATTTTGCGTC	maoC-like dehydratase, putative
Tb927.8.1440		ACCACTTTGTACAAGAAAGCTGGGTCTCGAGACATTCCACTCGCTCTCACC	maoC-like dehydratase, putative
Tb927.8.6970		ACAAGTTTGTACAAAAAAGCAGGCTAAGCTTTATTTACGCCGAATCGCCGA	3-methylcrotonyl-CoA carboxylase alpha subunit, putative
Tb927.8.6970		ACCACTTTGTACAAGAAAGCTGGGTCTCGAGTGGAGACAGTGACACGAACG	3-methylcrotonyl-CoA carboxylase alpha subunit, putative

Primers for Colony PCR

gRNAi forward	CGCTGACTTTCCAAGACCTC
gRNAi reverse	CAGATCGTCTTCACCCCCTA

SDM-79 media preparation for cell cultivation:

SDM-79 media	
SDM-79	25,5 g
DI water	1 L

* pH adjustment to 7,5 and filter sterilize. Then heat-inactivated fetal bovine serum and hemin solution was added to a concentration of 7,5 µg/mL

Hemin solution	
Hemin	50,0 mg
DI water	100 mL
1 N NaOH	1 mL

Reaction mix used for Gibson assembly:

Stuffer	50-100 ng per reaction (2x excess)
pTrypson	50-100 ng per reaction
Insert	3x fold excess
mQ water	1,15 µL
Gibbson Assembly Master mix	5 µL

PCR programs used:

Cracking program used for colony PCR

94°C	2’	
94°C	20’’	15x
65°C (-1°C per cycle)	30’’	
72°C	1’15’’	
94°C	20’’	20x
50°C	30’’	
72°C	1’15’’	
72°C	7’	
12°C	12’	

PCR conditions for colony PCR

96°C	5’
50°C	1’50’’
96°C	1’50’’
45°C	1’
96°C	1’
40°C	1’
4°C	2’

Composition of gels used for SDS-PAGE

Substance amounts for 1gel	Resolving gel (10 ml)	Stacking gel (6 ml)
Water	3.3 ml	4.35 ml
Acrylamide Mix	4.0 ml	1.0 ml
Tris buffer (1.5M)	2.5 ml	0.5 ml
SDS	0.1 ml	0.06 ml
APS	0.1 ml	0.06 ml
TEMED	0.004 ml	0.006 ml

* Tris Buffer: resolving gel pH: 6.8, stacking gel pH: 8.8

Antibodies used for Western Blots:

Primary antibody	Dilution	Secondary antibody	Dilution
anti-V5 made in mouse	1:1000	anti-mouse	1:1000
anti-HSP70 in mouse	1:1000	anti-mouse	1:1000
anti-APRT in rabbit	1:500	anti-rabbit	1:1000
Alpha Tubulin in mouse	1:1000	anti-mouse	1:1000

Solutions used for Western Blot:

Blotting buffer	
Water	700 mL
Methanol	200 mL
10x blotting buffer	100 mL

10x Blotting Buffer components for 2 liter	
192 mM Glycine	58 g
25 mM Tris	116 g
0,1% SDS	7,4 g

PBS + tween20	
Water	900 mL
10x PBS	100 mL
tween20	500 µL

Running Buffer	
Water	900 mL
10x running buffer	100 mL

10x Running Buffer components for 2 liter	
25 mM Tris	60 g
192 mM Glycine	288 g
0,1% SDS	20 g

Laemmli buffer (lysis buffer)

Reagent	Molecular weight	Concentration (M or %)
1x		
Tris base	121,14	0,0625 M
SDS	288,37	0,07 M (2%)
Glycerol	92,09	10%
2-mercapto-ethanol	78,13	5%
Bromophenol blue	691,94	-

List of used literature

Acosta, H., Burchmore, R., Naula, C., Gualdrón-López, M., Quintero-Troconis, E., Cáceres, A. J., ... & Quiñones, W. (2019). Proteomic analysis of glycosomes from Trypanosoma cruzi epimastigotes. *Molecular and biochemical parasitology*, *229*, 62-74.

Aslett, M., Aurrecoechea, C., Berriman, M., Brestelli, J., Brunk, B. P., Carrington, M., ... & Wang, H. (2010). TriTrypDB: a functional genomic resource for the Trypanosomatidae. *Nucleic acids research*, *38*(suppl_1), D457-D462.

Azevedo, F., Pereira, H., & Johansson, B. (2017). Colony PCR. In *PCR* (pp. 129-139). Springer, New York, NY.

Barrett, M. P., Burchmore, R. J., Stich, A., Lazzari, J. O., Frasch, A. C., Cazzulo, J. J., & Krishna, S. (2003). The trypanosomiases. *The Lancet*, *362*(9394), 1469-1480.

Bauer, S., & Morris, M. T. (2017). Glycosome biogenesis in trypanosomes and the de novo dilemma. *PLoS neglected tropical diseases*, *11*(4), e0005333.

Bílý, T., Sheikh, S., Mallet, A., Bastin, P., Pérez-Morga, D., Lukeš, J., & Hashimi, H. (2021). Ultrastructural Changes of the Mitochondrion During the Life Cycle of Trypanosoma brucei. *Journal of Eukaryotic Microbiology*, e12846.

Brun, R., Blum, J., Chappuis, F., & Burri, C. (2010). Human african trypanosomiasis. *The Lancet*, *375*(9709), 148-159.

Dean, S., Sunter, J. D., & Wheeler, R. J. (2017). TrypTag. org: a trypanosome genome-wide protein localisation resource. *Trends in parasitology*, *33*(2), 80-82.

Dean, S., Sunter, J., Wheeler, R. J., Hodkinson, I., Gluenz, E., & Gull, K. (2015). A toolkit enabling efficient, scalable and reproducible gene tagging in trypanosomatids. *Open biology*, *5*(1), 140197.

Gibson, D. G., Glass, J. I., Lartigue, C., Noskov, V. N., Chuang, R. Y., Algire, M. A., ... & Venter, J. C. (2010). Creation of a bacterial cell controlled by a chemically synthesized genome. *science*, *329*(5987), 52-56.

Gibson, D. G., Young, L., Chuang, R. Y., Venter, J. C., Hutchison, C. A., & Smith, H. O. (2009). Enzymatic assembly of DNA molecules up to several hundred kilobases. *Nature methods*, *6*(5), 343-345.

Gibson, D. G., Young, L., Chuang, R. Y., Venter, J. C., Hutchison, C. A., & Smith, H. O. (2009). Enzymatic assembly of DNA molecules up to several hundred kilobases. *Nature methods*, *6*(5), 343-345.

Güther, M. L. S., Urbaniak, M. D., Tavendale, A., Prescott, A., & Ferguson, M. A. (2014). High-confidence glycosome proteome for procyclic form Trypanosoma brucei by epitope-tag organelle enrichment and SILAC proteomics. *Journal of proteome research*, *13*(6), 2796-2806.

Kadri, K. (2019). Polymerase chain reaction (PCR): principle and applications. In *Synthetic Biology-New Interdisciplinary Science*. IntechOpen.

Mahmood, T., & Yang, P. C. (2012). Western blot: technique, theory, and trouble shooting. *North American journal of medical sciences*, *4*(9), 429.

Maier, R.M., Pepper, I.L., and Gerba, C.P. (2000) Environmental Microbiology. Academic Press, San Diego.

McAllaster, M. R., Sinclair-Davis, A. N., Hilton, N. A., & de Graffenried, C. L. (2016). A unified approach towards Trypanosoma brucei functional genomics using Gibson assembly. *Molecular and biochemical parasitology*, *210*(1-2), 13-21.

Panigrahi, A. K., Ogata, Y., Zíková, A., Anupama, A., Dalley, R. A., Acestor, N., ... & Stuart, K. D. (2009). A comprehensive analysis of Trypanosoma brucei mitochondrial proteome. *Proteomics*, *9*(2), 434-450.

Parsons, M. (2004). Glycosomes: parasites and the divergence of peroxisomal purpose. *Molecular microbiology*, *53*(3), 717-724.

Rajput, Y. S., & Sharma, R. (2011). SDS-PAGE–Principle and Applications. *Chemical Analysis of Value Added Dairy Products and Their Quality Assurance*, 81.

Schneider, A., & Ochsenreiter, T. (2018). Failure is not an option–mitochondrial genome segregation in trypanosomes. *Journal of cell science*, *131*(18).

Zíková, A., Verner, Z., Nenarokova, A., Michels, P. A., & Lukeš, J. (2017). A paradigm shift: The mitoproteomes of procyclic and bloodstream Trypanosoma brucei are comparably complex. *PLoS pathogens*, *13*(12), e1006679.